Extreme Mechanics Letters 27 (2019) 52–58

Contents lists available at ScienceDirect

Extreme Mechanics Letters

journal homepage: www.elsevier.com/locate/eml

Sew-free anisotropic textile composites for rapid design and manufacturing of soft wearable robots

Fionnuala Connolly [a], Diana A. Wagner [b], Conor J. Walsh [a,b], Katia Bertoldi [a,b,c,*]

[a] John A. Paulson School of Engineering and Applied Sciences, Harvard University, Cambridge, MA 02138, USA
[b] Wyss Institute for Biologically Inspired Engineering, Harvard University, Cambridge, MA 02138, USA
[c] Kavli Institute, Harvard University, Cambridge, MA 02138, USA

ARTICLE INFO

Article history:
Received 5 October 2018
Received in revised form 10 January 2019
Accepted 10 January 2019
Available online 17 January 2019

Keywords:
Soft actuator
Textile
Wearable robot

ABSTRACT

Textiles are promising materials to realize the next generation of pneumatic soft robots as they are lightweight, conformable, stretchable, and intrinsically anisotropic. Exploiting these properties, here we describe the fabrication and mechanical characterization of a new type of bending textile actuator. The actuator is fabricated using a lamination and layering process which eliminates the need for complex cut-and-sew procedures or the addition of components such as a bladder to contain air. We demonstrate the use of films to create air-impermeable textile composites and to alter the mechanical properties of the textiles, facilitating the design of actuators which exhibit complex deformation patterns. We mechanically characterize the textile composites and mathematically model their behavior. Finally, we show that our manufacturing and modeling methods facilitate the design of actuators tailored to specific functions, as demonstrated by our soft textile-based robotic glove.

1. Introduction

Inflatable actuators made of compliant elastomeric materials have attracted growing interest in recent years [1–3] and have enabled the design of soft wearable robots and assistive devices that can safely and effectively interact closely with humans [4–6]. However, one drawback of using elastomers is that their response is intrinsically isotropic. This necessitates the embedding of either complex architecture [7–9] or carefully oriented fibers [10,11] into the actuators, thus introducing the required anisotropy but also adding complexity to the system. Furthermore, while elastomeric soft actuators are very compliant, they can be too heavy and bulky for wearable robots and overly restrict the movement of joints even when the device is unpowered.

Textiles are promising materials to realize the next generation of soft wearable robots, as they are lightweight, conformable, stretchable, and intrinsically anisotropic. Because of their lightness, compliance, and low packing volume, textiles have already been utilized in a variety of inflatable structures, including airbags for car safety [12], temporary shelters [13,14], and soft actuators which provide linear and rotary motions [15,16]. However, these structures do not take advantage of the stretchability and anisotropy of textiles, and their inflated configuration is completely determined by their initial shape rather than the mechanical stretch afforded by knit textiles. Only very recently it has been shown that the intrinsic anisotropy and stretchability of textiles can be exploited to create bending actuators with very simple geometry [17]. This effort, however, represents only the first step towards textile-based wearable soft robots. The fabrication of the actuators via a cutting and sewing process is not only labor-intensive and time-consuming, but also introduces weak points into the textile where failure is more likely to occur during inflation. Moreover, since actuation is achieved by inflating a thermoplastic elastomer balloon inside the textile pocket, the response is often not repeatable due to inconsistencies in balloon insertion and movement of the balloon inside the pocket. In order to realistically bring the great potential of textiles to wearable soft robots, there is the need not only to identify new approaches for quickly manufacturing actuators that perform reliably and repeatably, but also to develop mathematical models to guide their design.

Here, we combine experimental and analytical tools to realize textile-based soft inflatable actuators that can be integrated into a glove to assist impaired individuals in performing activities of daily living [18,19]. Our bending actuators fully exploit the anisotropic properties of highly stretchable textiles (Fig. 1a) and are rapidly designed by employing a mathematical model that enables us to identify the geometric parameters resulting in the desired motion for a given application (Fig. 1b). Moreover, a manufacturing approach which involves laminating the textiles with a thermoplastic air-impermeable film and using heat to bond them enables the

* Corresponding author at: John A. Paulson School of Engineering and Applied Sciences, Harvard University, Cambridge, MA 02138, USA.
E-mail addresses: walsh@seas.harvard.edu (C.J. Walsh), bertoldi@seas.harvard.edu (K. Bertoldi).

https://doi.org/10.1016/j.eml.2019.01.007
2352-4316/

rapid fabrication of different actuator designs that do not rely on a separate balloon to achieve inflation (Fig. 1c). With these new manufacturing and modeling approaches, we design actuators with articulation which imitate the motion of a finger and can be integrated into an assistive glove (Fig. 1d). Notably, our manufacturing and modeling strategies are not limited to the specific cases presented here, but could be applied to a range of assistive and wearable robots for both upper and lower extremity applications.

2. Textile selection and modeling

We start by noting that to produce the required bending motion while keeping the actuator as low-profile as possible along the top of the finger, the top part of the actuator calls for a textile which stretches significantly in one direction and stretches minimally in the perpendicular direction, while for the bottom part we need a textile which stretches less in all directions. We also note that while the bottom textile should not stretch very much, it should still have some extensibility — this allows us to incorporate the actuator into wearable devices which can stretch as a person moves. Furthermore, to enable pneumatic actuation we need to make the textiles impermeable to air. This can be achieved by coating the textiles with a thermoplastic polyurethane film (3918, Bemis Company, Inc.), which not only makes the textiles air impermeable, but also preserves their anisotropic properties and does not overly inhibit their extensibility (see Figure S1).

Next, we use mechanical testing to identify commercially available textiles with the ideal mechanical properties. More specifically, we conduct uniaxial and equibiaxial tension tests on different textile-film composites (see Supporting Information for more details). We use knitted textiles since their looped structure enables high levels of stretch and recovery. Knits have two distinct directions referred to as the wale (parallel to the direction of manufacturing) and the course (perpendicular to the direction of manufacturing). For the top part of the actuator, we choose a knit whose structure permits high stretch in the wale direction while restricting stretch in the course direction (see Fig. 2c). For the bottom, we choose a knit which is significantly stiffer than the top knit in both the course and wale directions (see Fig. 2d). Finally, it is important to note that the mechanical response of the selected textiles can be nicely captured using a hyperelastic anisotropic continuum model such as the Holzapfel–Gasser–Ogden model [20], whose strain energy is given by

$$W = C(I_1 - 3) + \frac{k_1}{2k_2}\left(e^{k_2(I_4-1)^2} - 1\right). \quad (1)$$

In the equation above, C, k_1, k_2 are material parameters, $I_1 = \mathrm{tr}(\mathbf{F}\mathbf{F}^T)$ and $I_4 = \mathbf{FM}\cdot\mathbf{FM}$, $\mathbf{F}$ being the deformation gradient and $\mathbf{M}$ denoting the stiffest direction of the textile in the undeformed configuration (see Supporting Information for more details). We find that the response of the top layer is best captured using $C = 0.64$ MPa, $k_1 = 0.12$ MPa, and $k_2 = 0.52$ (see Fig. 2c), while for the bottom layer $C = 0.99$ MPa, $k_1 = 0.017$ MPa, and $k_2 = 1.1$ lead to the best match (see Fig. 2d).

3. Actuator fabrication

Having identified two textile-film composites with ideal mechanical properties, we now combine them to make inflatable actuators. To this end, we take advantage of the fact that the film which we applied to the textiles to make them air-impermeable can bond to itself and we use a heat press (Digital Knight DK20S) to put the two composite layers together, eliminating the need to sew a complex seam. To form an airtight textile pocket, we place between the two layers a water-soluble polymer (Sulky Ultra Solvy Stabilizer, a polyvinyl alcohol) which has been cut (using a Versa laser) into the shape of the desired actuator chamber. The polymer does not adhere to the film during heating and, when the bonding process is complete, can simply be dissolved using water. The actuator is finished by inserting a tube and gluing it in place (see Supporting Information for more details).

We start by fabricating bending actuators with a rectangular chamber of width W and length L (the chamber also has an additional taper towards the tubing and is rounded at the distal end — see Fig. 3a). To quantify the deformation of our actuators during inflation, we use a camera (Canon EOS Rebel T5i) and extract their outer edge (in the region of the chamber of initial length L) from the recorded images via edge detection. By finding the circular arc which best fits the edge of length l_t, we can identify the radius of curvature of the actuator ρ and the bend angle $\psi = l_t/\rho$. Moreover, by tracking the white lines located at the two ends of the chamber (indicated by the red boxes in Fig. 3d) via digital image processing we can monitor the radius of the actuator r_i (see Supporting Information).

In Fig. 3e we report the evolution of the bend angle per unit length (ψ/L) and of the change in radius (r_i/R_i with $R_i = W/\pi$) as a function of the applied pressure for three actuators with length $L = 110$ mm and width $W = 10$ mm (green markers), 20 mm (blue markers), and 30 mm (black markers). All actuators are initially flat. We find that as the inflation starts (i.e. for very small values of applied pressure - Fig. 3e) the bend angle ψ of all three actuators remains almost zero, while the radius r_i rapidly increases until $r_i/R_i = 1$. At this point the actuators take on a cylindrical shape with radius $R_i = W/\pi$ (see Fig. 3b). However, as the pressure increases, the textiles begin to stretch and the actuators start to bend, taking on the shape of a toroidal segment (Fig. 3c and d). We see that the actuator with $W = 10$ mm deforms the most, reaching $\psi = 1.5°$/mm at a pressure of 250 kPa. In contrast, the actuators with widths $W = 20$ mm and 30 mm deform less and can sustain lower values of pressure.

4. Actuator modeling

The experimental results of Fig. 3c indicate that the response of the actuators can be tuned by varying their geometry. To rapidly navigate the design space and identify actuator geometry leading to the desired response for a particular application, we develop a mathematical model based on nonlinear elasticity. Previous models of pneumatic soft actuators often relied on finite element analysis which gives accurate results but is time-consuming [21–23]. Analytical models were developed as an alternative, but relied on the assumption of zero deformation in the radial direction [6,24]. Such assumption is clearly violated by our textile-based actuators, necessitating a new modeling approach. Taking inspiration from the volume maximization strategy recently proposed to model elastomeric fiber-reinforced actuators [25], here we use strain energy minimization to predict the actuator deformation (see Supporting Information for more details). More specifically, guided by our experiments, we assume that the actuator starts from a cylindrical configuration with inner radius $R_i = W/\pi$ and length L, and inflates to the shape of a toroidal segment with major radius ρ, minor radius r_i, and length l_t (neglecting the ends of the actuator). Since the actuator consists of two materials, which deform differently, one more parameter k is introduced to relate the extension in the circumferential direction of the top layer to that of the bottom one. Finally, to simplify the model, we assume that all materials in the actuator are incompressible, an assumption which we validated using finite element analysis (see Supporting Information for more details). Under these assumptions, the strain energy U of the actuator can be written as:

$$U = \int_0^L \int_{-\frac{\pi}{2}}^{\frac{\pi}{2}} \int_{R_i}^{R_o} W^{(b)} R\,\mathrm{d}R\mathrm{d}\Theta\mathrm{d}Z + \int_0^L \int_{\frac{\pi}{2}}^{\frac{3\pi}{2}} \int_{R_i}^{R_o} W^{(t)} R\,\mathrm{d}R\mathrm{d}\Theta\mathrm{d}Z,$$

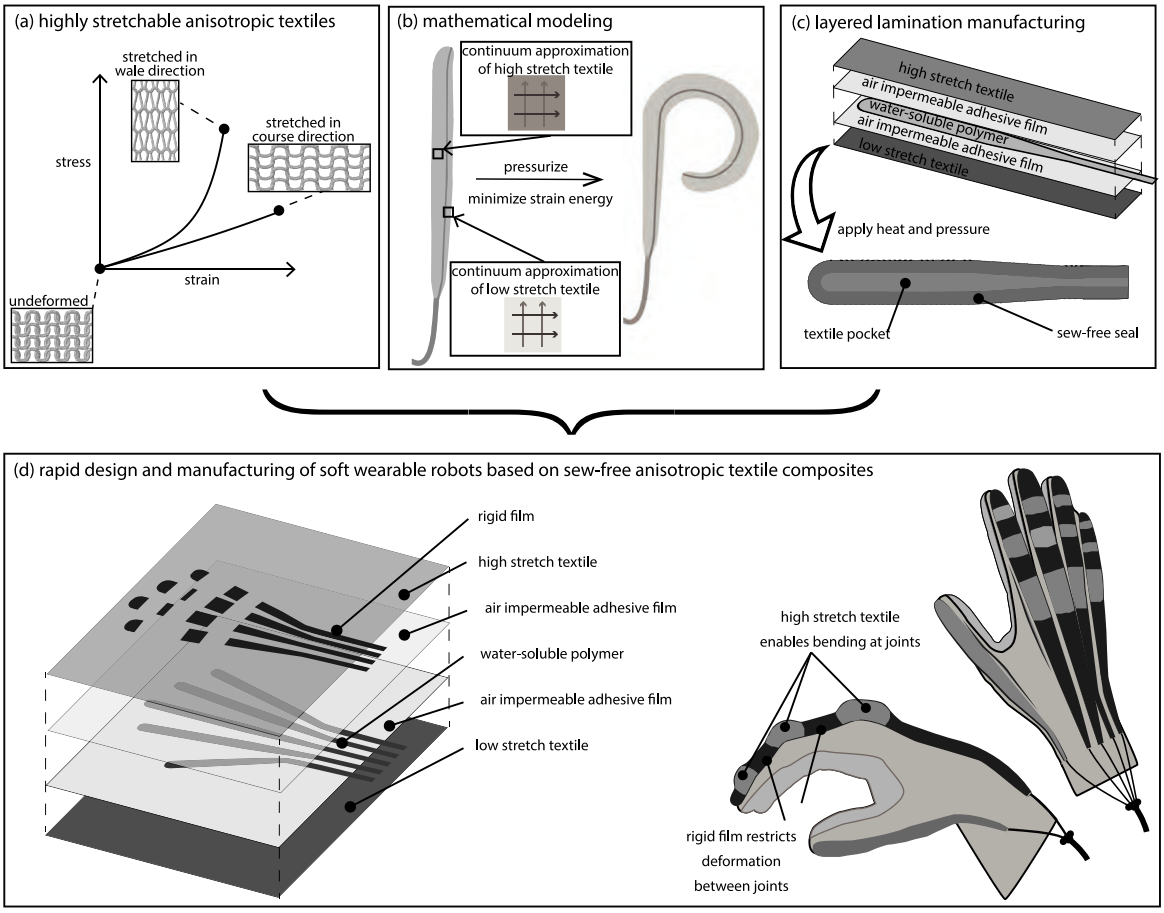

Fig. 1. (a) Knitted textiles show highly anisotropic behavior under uniaxial tension. (b) By modeling textiles as homogeneous anisotropic continua, we can develop models of bending textile actuators. (c) Using lamination and layering, we can fabricate actuators quickly and easily. (d) Manufacturing and modeling approaches can easily be scaled to more complex designs.

(2)

where $W^{(b)}(\Theta)$ and $W^{(t)}(\Theta)$ are the strain energy densities of the bottom and top textiles (given by Eq. (1)), R, Θ and Z are the radial, circumferential, and axial coordinates in the initial configuration, R_i and R_o are the initial inner and outer radii of the actuator, and L is the initial length of the actuator. Since the volume enclosed by a toroidal segment is

$$V = \pi r_i^2 \frac{l_t}{\rho + r_i}\rho, \tag{3}$$

given a supplied volume $V_{supplied}$ inside the actuator, we then solve for (ρ, r_i, l_t, k) by minimizing the strain energy U (via the constrained nonlinear solver fmincon in Matlab) subject to the constraint $V_{supplied} = V$. Finally, we use the Cauchy equilibrium equations to relate the deformation to the internal pressure P (see Supporting Information for details):

$$P = \frac{1}{2\pi}\int_{-\frac{\pi}{2}}^{\frac{\pi}{2}}\int_{r_i}^{r_o}\frac{\sigma_{\theta\theta}^{(b)}(\Theta) - \sigma_{rr}^{(b)}}{r}\mathrm{d}r\mathrm{d}\Theta + \frac{1}{2\pi}\int_{\frac{\pi}{2}}^{\frac{3\pi}{2}}\int_{r_i}^{r_o}\frac{\sigma_{\theta\theta}^{(t)}(\Theta) - \sigma_{rr}^{(t)}}{r}\mathrm{d}r\mathrm{d}\Theta, \tag{4}$$

where $\sigma^{(\alpha)} = -p\mathbf{I} + \frac{1}{\det\mathbf{F}}\frac{\partial W^{(\alpha)}}{\partial \mathbf{F}}\mathbf{F}^T$ is the Cauchy stress (p is a hydrostatic stress, I is the identity matrix, and $\alpha \in \{t, b\}$ refers to the top and bottom textiles). In Fig. 3e, we compare the predictions of this model (continuous lines) to experimental results (markers) for the three considered different geometries. We see a reasonably good match between model and experiment, with discrepancies most likely due to the constitutive models for the textiles not picking up all of the complexities of the textile behavior and to the assumption that the actuator cross-section is perfectly circular.

5. Application to assistive glove

Having identified tools for rapidly modeling and manufacturing textile actuators, we now demonstrate that these methods enable us to design a wearable device which assists with grasping. It has been shown that soft robotic gloves can help people who have hand impairments with performing activities of daily living [18,19,26,27]. This idea has been explored in detail for elastomeric actuators [18], but more recently, textile actuators have been proposed as an alternative [17] as they are easier to integrate into wearable devices. Furthermore, textiles are more lightweight than elastomers, making the device transparent when not actuated – this means it is more comfortable to wear and does not impede movement. While previous work has shown that textile actuators could successfully be used in a soft robotic glove [19], here we show that our new manufacturing and modeling methods facilitate faster and simpler fabrication of the device, as well as the design of actuators which more accurately mimic finger motion.

We first note that the textile actuators presented in Fig. 3 are not ideal to mimic finger motion, since they have constant bending curvature, whereas fingers bend at discrete locations (i.e. joints). To produce actuators capable of matching the motion of the fingers, we require the portions of the actuator which will be located at the joints to bend upon inflation, while those in between should resist deformation. Notably, these alternating bending and straight

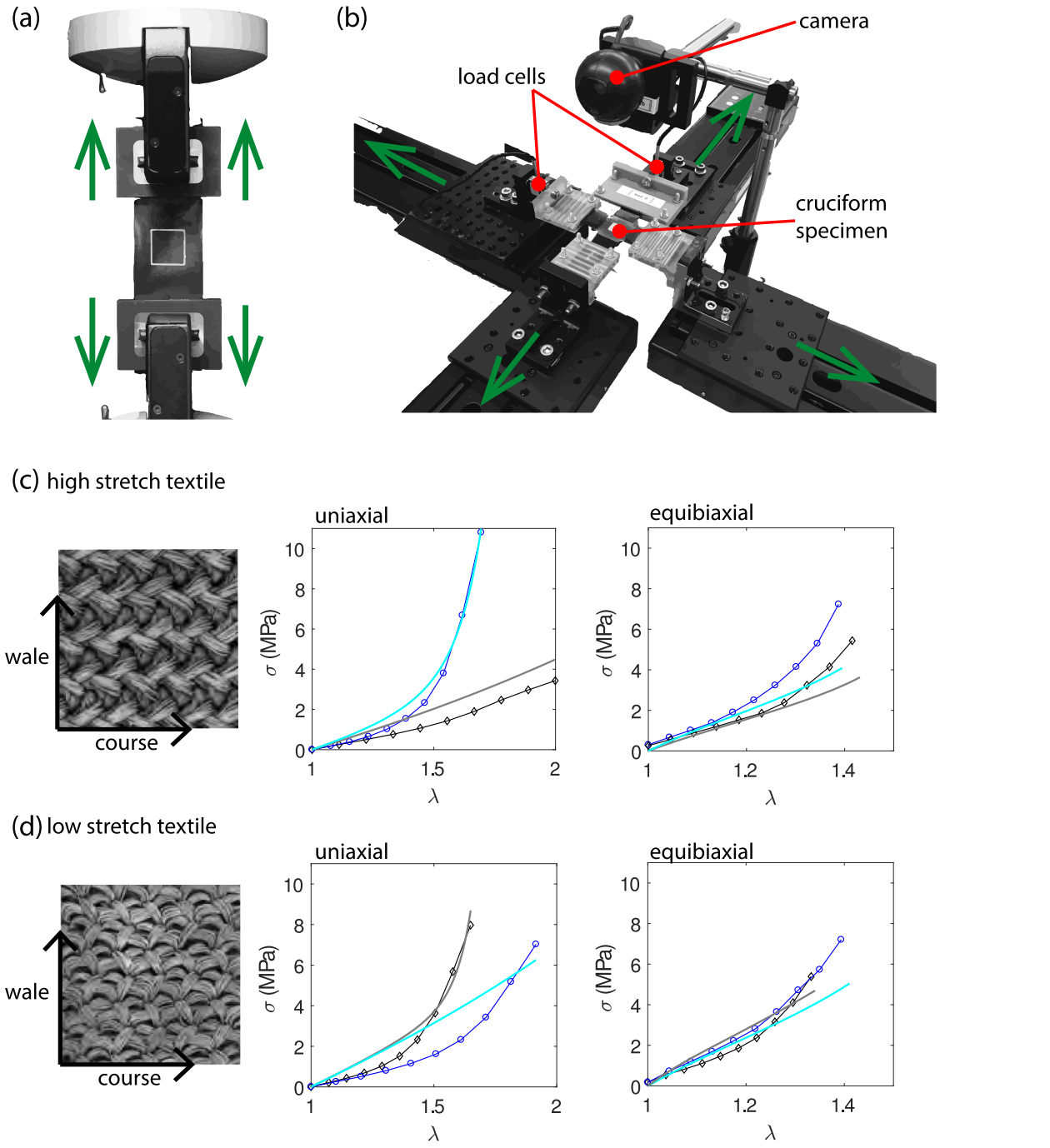

Fig. 2. (a) Uniaxial tensile test setup (b) Biaxial tensile test setup (c) SEM image, experimental data, and best-fit model for the laminated Raschel knit (24710, Darlington Fabrics) (d) SEM image, experimental data, and best-fit model for the laminated Tricot knit (26210, Darlington Fabrics).

segments can be realized with a single pocket (so that the actuator has only a single pressure input), by applying a stiff polyamide film (4220, Bemis Company, Inc.) to alternating portions of the actuator to significantly increase its stiffness in those areas. Thus, such articulated actuators can be manufactured following the same procedure as before, simply adding an extra step where we laminate the actuators with the stiff film in alternating areas (Fig. 4b). However, identifying the actuator width and the lengths of the bending and straight segments is challenging, as there are a few requirements which must be fulfilled. More specifically, we want the actuator (*i*) to be as narrow as possible, to ensure it remains low-profile when inflated (but it must still be wide enough to enable easy fabrication and provide adequate force); (*ii*) to achieve the target configuration at a low pressure, to ensure safe operation and minimize hardware requirements; (*iii*) to have bending segment lengths which are as short as possible (to fit over the joints). Assuming that there are no interactions between bending and straight segments, we can use our analytical model to identify actuators capable of achieving the target configuration while satisfying all these requirements. To this end, in Fig. 4c we report the bend per unit length as a function of initial actuator width and applied pressure as predicted by our analytical model for a homogeneous bending segment. We see that

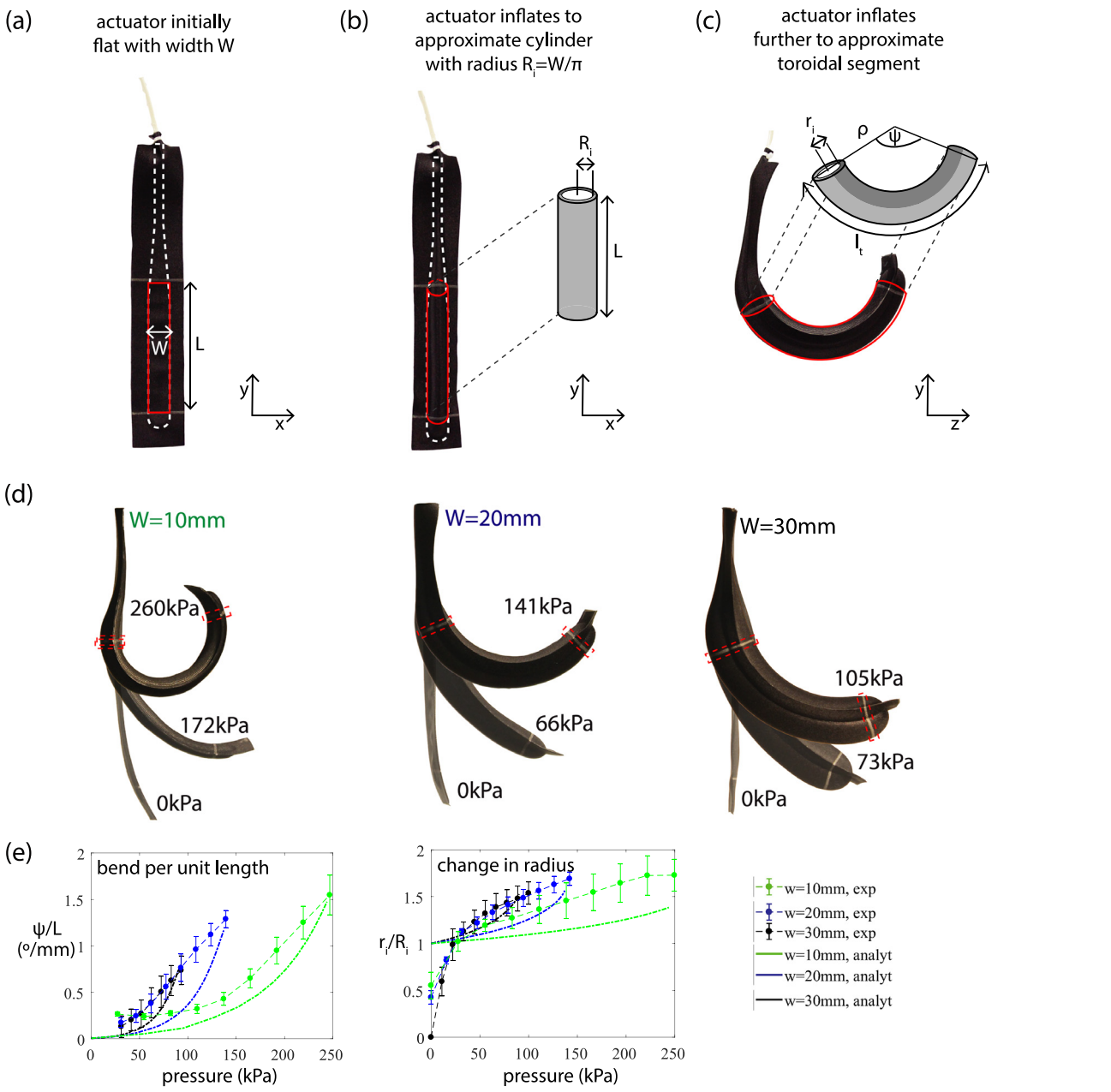

Fig. 3. (a)–(c) Illustration of model parameters (d) Photographs of actuators with different widths at different actuation pressures. (e) Comparison of experimental results and model predictions of actuator deformation.

at any given pressure, wider actuators yield greater bend per unit length (ψ/L). Moreover, we find that for each actuator width, there is a critical pressure above which the model breaks down due to a ballooning instability in the constitutive models (see white area in Fig. 4c). Such instability clearly limits the maximum pressure at which we can operate.

To demonstrate the power of our modeling approach, we choose an everyday task – picking up a glass or bottle – and use the predictions of Fig. 4c to design actuators that mimic the grasping motion used for that task. Given the average joint angles for grasping a cylindrical object of diameter 50.8 mm [28] and the average finger dimensions for a large-sized hand (see Fig. 4a and Supporting Information), we can identify the required actuator configurations for each of the fingers (index, middle, ring, and little). Focusing on a middle finger with total length of 194 mm, we find that an actuator of width 11.5 mm with bending segments of length 27 mm, 25 mm, and 21 mm reaches the target configuration at a pressure of 240 kPa (Fig. 4d), satisfying all of our requirements. In Fig. 4e we show the fabricated actuator based on this design when inflated to a pressure of 240 kPa, with its target shape overlaid. We see that the actuator behaves as expected, with only a slight difference between the target configuration and the actual configuration. This difference is most likely due to the inaccuracies of the model (as outlined above) and also due to our assumption that the straight segments do not affect the deformation of the bending segments (we can see in Fig. 4e that the radius of a bending segment has to decrease a lot at its edges in order to match the radius of the straight segments). However, the discrepancy between the target configuration and the actual configuration is not large enough that we would expect it to affect the functionality of a soft robotic glove. Finally, while in Fig. 4 we show results only for the middle finger, the index, ring, and little finger actuators were designed similarly (see Supporting Information).

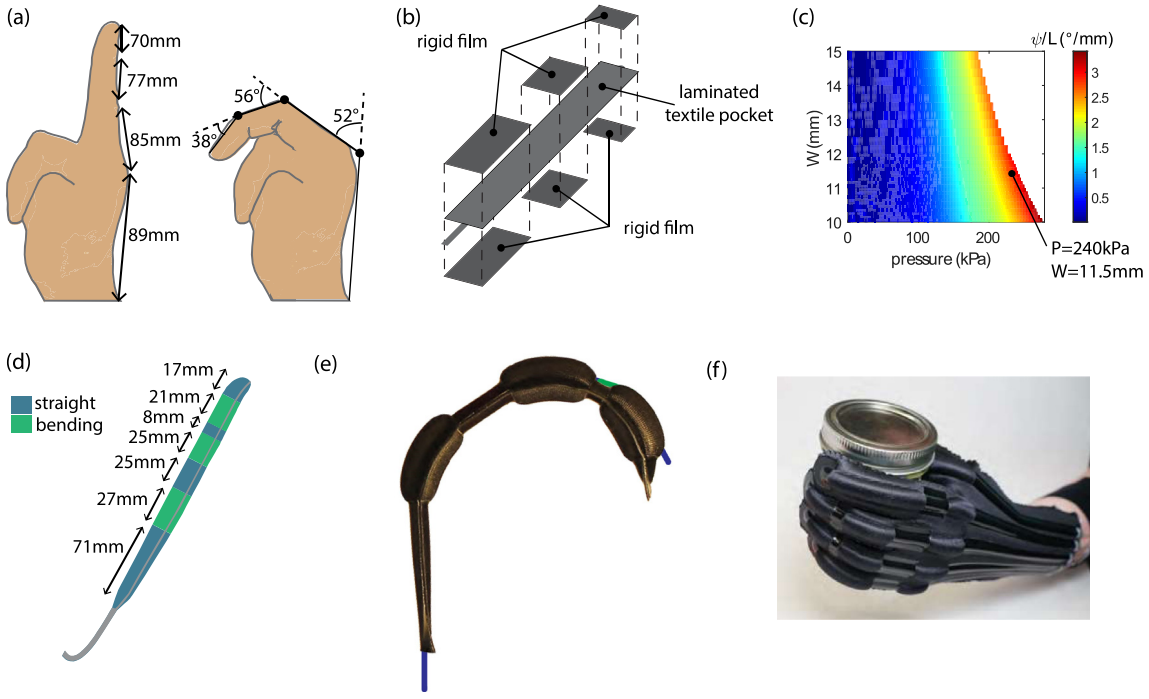

Fig. 4. (a) Middle finger joint angles and lengths (b) Applying rigid film to the outside of the actuator yields the straight segments (c) Contour plot showing bend angle per unit length as a function of actuator width and applied pressure (d) Middle finger actuator design (e) Middle finger actuator at 240 kPa, overlaid with target configuration (f) Assistive glove pressurized to 240 kPa.

Next, we show that the articulated actuators we have designed can be integrated into an assistive glove. Rather than individually fabricating an actuator for each finger, we use our layered manufacturing approach to make the device in a single piece (see Supporting Information). Since the geometry here is more complex than that of the individual actuators, we use an alignment board and pins to ensure that the layers line up correctly. As before, we start by laminating both the high stretch and low stretch textiles. We then seal the laminated textiles together to create a glove-shaped device with five embedded air chambers. We add rigid film to the top and bottom of the device to create articulation for each of the fingers, and we insert tubing to provide an air supply to each of the actuators. Lastly, we make the device wearable by sewing it onto a large-size glove (Shima Seiki USA). For the index, middle, ring, and little fingers, we use the articulated actuator designs identified in the previous section. Differently, for the thumb we use just a simple bending actuator, since the actuators presented here are not sufficient to replicate its ability to move out of plane as it bends. Note that since the glove is fabricated all in one piece (as shown in Fig. 1d), the middle finger is aligned with the wale direction of the textile, as in the model, but the index, ring, and little fingers are at a slight angle to the wale. We ran a finite element simulation to compare the behavior of an actuator aligned with the wale to the behavior of one at an angle of 10° and found that their behavior was quite similar, and therefore this angle did not affect the functionality of the glove (see Supporting Information).

Pressurizing all five of the actuators in the glove to 240 kPa, we see that the glove produces a grasping motion, enabling the wearer to grasp a jar (Fig. 4f). Notably, since the articulated actuators have been designed to mimic finger motion, they distribute pressure more evenly over the fingers than simple bending actuators which have constant curvature and produce a motion which is further from the natural motion of the fingers (see Supporting Information). Moreover, while the glove stiffens and applies forces to the wearer when it is actuated, the compliance and flexibility of its constitutive materials make it transparent when not actuated (see Supplementary Video).

6. Conclusions

In summary, we have presented new manufacturing and analytical methods for rapidly fabricating and modeling textile actuators. In particular we have shown how to laminate highly stretchable textiles to make them air-impermeable and heat-sealable. We have mechanically characterized these textile-film composites and used the characterization results in an analytical model which predicts the quasi-static behavior of the actuators. Future work on this project will include modeling the time-dependent response of the actuators.

The manufacturing and modeling methods presented here allow for the rapid iteration of actuator designs, as the modeling process tells us the effect of changing actuator geometry, while the manufacturing process allows us to quickly investigate the effect of using different materials (such as different textiles or films with different properties). Our manufacturing process can easily be scaled to produce devices with more complex geometries, giving these actuators potential to be used in a wide range of wearable and assistive devices. These devices could aid people who have suffered injuries which impair their ability to perform activities of daily life, or could be used in factories to reduce work-related musculoskeletal injuries.

Acknowledgments

The authors thank Dr. S. Liberatore, E. Hajiesmaili, and Dr. A. Rafsanjani for assistance with biaxial testing and Dr. J. Weaver for assistance with SEM images. This work was supported by National Science Foundation, United States Awards DMR-1420570 (Materials Research Science and Engineering Center) and EFRI C3 SoRo 1830896.

Competing interests

The authors declare that they have no competing financial interests.

Appendix A. Supplementary data

Supplementary material related to this article can be found online at https://doi.org/10.1016/j.eml.2019.01.007.

References

[1] P. Polygerinos, N. Correll, S.A. Morin, B. Mosadegh, C.D. Onal, K. Petersen, M. Cianchetti, M.T. Tolley, R.F. Shepherd, Soft robotics: Review of fluid-driven intrinsically soft devices; manufacturing, sensing, control, and applications in human-robot interaction, Adv. Eng. Mater. 19 (12) (2017).
[2] D. Rus, M.T. Tolley, Design, fabrication and control of soft robots, Nature 521 (2015) 467–475.
[3] C. Majidi, Soft robotics: A perspective - current trends and prospects for the future, Soft Robot. 1 (2013) 5–11.
[4] T. Noritsugu, M. Takaiwa, D. Sasaki, Power assist wear driven with pneumatic rubber artificial muscles, Int. Conf. Mechatronics Mach. Vis. Pract. (2008) 539–544.
[5] Y.L. Park, J. Santos, K.C. Galloway, E.C. Goldfield, R.J. Wood, A soft wearable robotic device for active knee motions using flat pneumatic artificial muscles, IEEE Int. Conf. Robot. Autom. (2014) 4805–4810.
[6] P. Polygerinos et al, Modeling of soft fiber-reinforced bending actuators, IEEE Trans. Robot. 31 (2015) 778–789.
[7] O.C. Jeong, S. Kusuda, S. Konishi, All pdms pneumatic balloon actuators for bidirectional motion of micro finger, in: 18th IEEE International Conference on Micro Electro Mechanical Systems, 2005, pp. 407–410.
[8] F. Ilievski, A.D. Mazzeo, R.F. Shepherd, X. Chen, G.M. Whitesides, Soft robotics for chemists, Angew. Chem. Int. Edn 50 (8) (2011) 1890–1895.
[9] S. Wakimoto, K. Suzumori, K. Ogura, Miniature pneumatic curling rubber actuator generating bidirectional motion with one air-supply tube, Adv. Robot. 25 (2011) 1311–1330.
[10] K. Suzumori, S. Iikura, H. Tanaka, Flexible microactuator for miniature robots, IEEE MEMS (1991) 204–209.
[11] K.C. Galloway, P. Polygerinos, C.J. Walsh, R.J. Wood, Mechanically programmable bend radius for fiber-reinforced soft actuators, Int. Conf. Adv. Robot. (2013) 1–6.
[12] J.W. Hetrick, Safety cushion assembly for automotive vehicles. U.S. patent 2649311A, Aug 05 1952.
[13] W.A. Bary, Inflatable structure. U. S. patent 2837101A, Apr 28 1955.
[14] E.C. Fink, Inflatable tent structure. U. S. patent 3055379A, Jul 16 1959.
[15] A. Mettam, Inflatable Servo Actuators, Technical Report, Ministry of Aviation, Aeronautical Research Council, 1964.
[16] S. Sanan, P.S. Lynn, S.T. Griffith, Pneumatic torsional actuators for inflatable robots, J. Mech. Robot. 6 (3) (2014).
[17] L. Cappello, K.C. Galloway, S. Sanan, D.A. Wagner, R. Granberry, S. Engelhardt, F.L. Haufe, J.D. Peisner, C.J. Walsh, Exploiting textile mechanical anisotropy for fabric-based pneumatic actuators, Soft Robot. 5 (5) (2018).
[18] P. Polygerinos, Z. Wang, K.C. Galloway, R.J. Wood, C.J. Walsh, Soft robotic glove for combined assistance and at-home rehabilitation, Robot. Auton. Syst. 73 (2015) 135–143.
[19] L. Cappello, J.T. Meyer, K.C. Galloway, J.D. Peisner, R. Granberry, D.A. Wagner, S. Engelhardt, S. Paganoni, C.J. Walsh, Assisting hand function after spinal cord injury with a fabric-based soft robotic glove, J. Neuroeng. Rehabil. 15 (1) (2018) 59.
[20] G.A. Holzapfel, T.C. Gasser, R.W. Ogden, A new constitutive framework for arterial wall mechanics and a comparative study of material models, J. Elast. 61 (2000) 1–48.
[21] K. Suzumori, S. Endo, T. Kanda, N. Kato, H. Suzuki, A bending pneumatic rubber actuator realizing soft-bodied manta swimming robot, IEEE Inc. Conf. Robot. Autom. (2007) 4975–4980.
[22] Y. Elsayed, A. Vincensi, C. Lekakou, T. Geng, C.M. Saaj, T. Ranzani, M. Cianchetti, A. Menciassi, Finite element analysis and design optimization of a pneumatically actuating silicone module for robotic surgery applications, Soft Robot. 1 (4) (2014) 255–262.
[23] P. Moseley et al, Modeling, design, and development of soft pneumatic actuators with finite element method, Adv. Eng. Mater. 18 (6) (2015) 978–988.
[24] F. Connolly, C.J. Walsh, K. Bertoldi, Automatic design of fiber-reinforced soft actuators for trajectory matching, Proc. Natl. Acad. Sci. 114 (1) (2017) 51–56.
[25] G. Singh, G. Krishnan, A constrained maximization formulation to analyze deformation of fiber reinforced elastomeric actuators, Smart Mater. Struct. 26 (6) (2017).
[26] T. Noritsugu, Pneumatic soft actuator for human assist technology, in: Proc JFPS Int Symposium on Fluid Power, 2005, pp. 11–20.
[27] L. Connelly, Y. Jia, M.L. Toro, M.E. Stoykov, R.V. Kenyon D.G. Kamper, A pneumatic glove and immersive virtual reality environment for hand rehabilitative training after stroke, IEEE Trans. Neural Syst. Rehabil. Eng. 18 (2010) 551–559.
[28] J.W. Lee, K. Rim, Measurement of finger joint angles and maximum finger forces during cylinder grip activity, J. Biomed. Eng. 13 (1991) 152–162.